LASER TECHNOLOGIES

PACS numbers: 81.05.Je; 81.05.Kf; 81.05.Mh; 42.62.Cf; 42.79. – e
DOI: 10.1070/QE2007v037n01ABEH008992

Laser amorphisation of glass ceramics: basic properties and new possibilities for manufacturing microoptical elements

V.P. Veiko, K.K. Kieu

***Abstract*. The laser amorphisation of glass ceramics (LAGC) is studied by optical pyrometry and video recording. The mechanism of local LAGC as a structural phase transition determined by the temperature kinetics in the laser-irradiated region is proposed. The ranges of the power density and exposures to the 10.6-μm IR radiation required for amorphisation of the typical glass ceramics, a $SiO_2 - Al_2O_3 - CaO - MgO - TiO_2$ sital are determined. It is shown that LAGC can be used to fabricate a number of miniature optical elements such as lenses, lens rasters, light guides and waveguides, etc.**

Keywords: *glass ceramics, laser amorphisation, microoptical elements*.

1. Introduction

Infrared radiation of a CO_2 laser can induce a variety of physical processes in glasses and glass ceramics, which result in the formation of local regions with modified optical parameters [1]. The most important from them are presented in Fig. 1.

Most of these phenomena have the thermal nature related to the fundamental absorption of the 10.6-μm IR radiation (the Bouguer coefficient is $\alpha = 8 \times 10^3$ cm^{-1}) in glasses and ceramics accompanied by the dissipation of the absorbed energy. The local nature of heating and a large temperature gradient along with high heating and cooling rates give rise to a new kinetics of structural variations and new possibilities for the fabrication of microoptical elements, and sometimes unknown optical materials [1].

A spectacular example of laser action on glass materials is the laser amorphisation of glass ceramics (LAGC). Glass ceramics (GCs)* represent a broad class of materials with a dense microcrystalline structure containing very small randomly oriented crystals and devoid of porosity. Because of their microcrystalline structure, GCs strongly scatter light and are opaque in the visible region despite weak absorption. These materials strongly absorb light in the mid-IR range between 5 and 10 μm, the Bouguer coefficient α in this range being $10^5 - 10^6$ cm^{-1}.

It was found that local laser heating drastically reduces light scattering in the visible range (Fig. 2) probably due to the melting of microcrystals and subsequent 'freezing' of the produced amorphous phase [1, 2].

This hypothesis was confirmed by observing X-ray diffraction from the initial structure and laser-induced structures (Fig. 3) [2]. One can see from Fig. 3 that the GC microcrystalline structure is mainly transformed to the amorphous phase, which is in turn reversible.

As a result, a transparent 'window' is formed in the laser-irradiated region of a sample against the background of the opaque initial material. In addition, the amorphous phase produced by the laser has a greater specific volume than the initial closer-packed microcrystalline phase. As a result, the macroscopic volume of the irradiated material increases and the irradiated region acquires a lens-like shape.

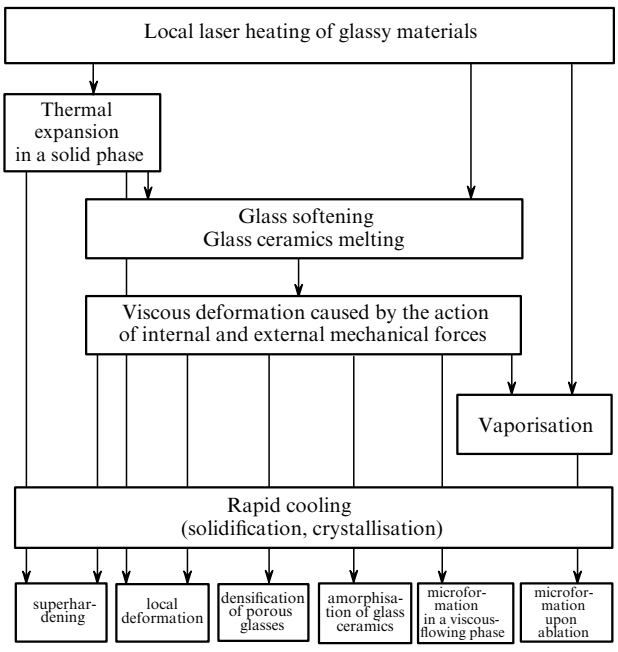

Figure 1. Scheme of laser-induced physical processes in glasses and glass ceramics.

*These materials are often called 'sitals' in Russian scientific literature.

V.P. Veiko, K.K. Kieu St. Petersburg State University of Information Technologies, Mechanics and Optics, Kronverkskii prosp. 14, 197101 St. Petersburg, Russia;
e-mail: veiko@lastech.ifmo.ru, khanh@lastech.ifmo.ru

Received 25 April 2005; revision received 28 May 2006
Kvantovaya Elektronika **37** (1) 92 – 98 (2007)
Translated by M.N. Sapozhnikov

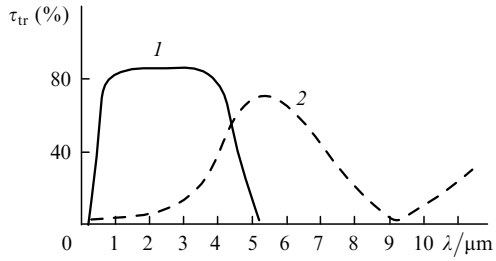

Figure 2. Transmission spectrum of ST-50-1 sital before (*1*) and after (*2*) laser amorphisation.

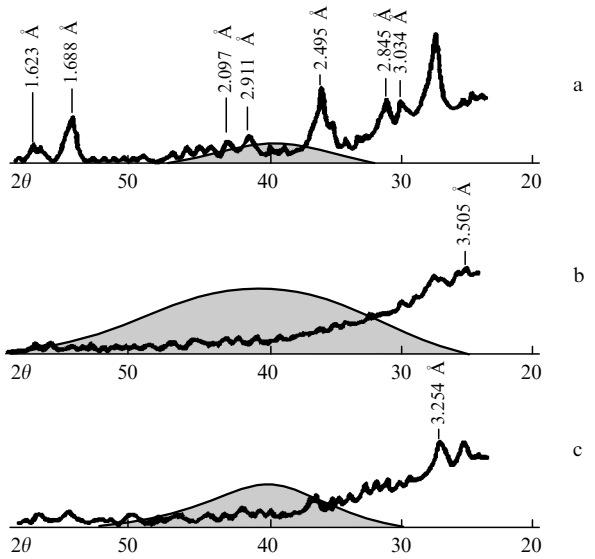

Figure 3. X-ray diffraction patterns of ST-50-1 sital before (a) and after (b) laser irradiation (laser amorphisation), and after repeated irradiation (partial crystallisation) (c). The peaks at 1.688, 2.495, and 3.254 Å belong to rutile (α-TiO_2), the 3.505-Å peak is typical for amorphous sital, the halo corresponds to the typical amorphous phase of SiO_2; the rest of the peaks belong to cordierite ($2MgO{\cdot}2Al_2O_3{\cdot}5SiO_2$).

It is clear from general considerations that the GC cooling (and heating) rate plays a decisive role in amorphisation (and crystallisation) processes. However, nobody has measured so far the temperature variation rate during laser irradiation of GCs. At the same time, it is the study of this question that can explain anomalously high rates of laser-induced structural modifications and can help to determine the technological processes of formation of optical elements.

In this paper, we studied the kinetics of laser-induced phase transitions by the methods of pyrometry and video recording and obtained quantitative data on the development of these processes.

2. Kinetics of laser-induced structural phase transformations in glass ceramics

The most informative parameters of laser-induced structural phase transformations are: (i) the temperature kinetics, especially the heating and cooling rates, which determine the formation of new phases and their stability and (ii) the movement of the amorphisation front caused by the appearance of the boundary and the movement of the transparency front in the initial sample.

We used ST-50-1 sital of the composition (mass %): 60.5 % of SiO_2, 13.5 % of Al_2O_3, 8.5 % of CaO, 7.5 % of MgO, and 10 % of TiO_2; here, the main components are rutile (α-TiO_2) and cordierite ($2MgO{\cdot}Al_2O_3{\cdot}5SiO_2$) microcrystals. Samples in the form of 0.3 – 1-mm thick plates were irradiated by a stabilised 50-W cw CO_2 laser. The size of the laser-irradiated region was varied between 0.5 and 2 mm, and the laser radiation power density on samples did not exceed 5×10^7 W m^{-2}.

The temperature kinetics (temperature and the rate of its variation) was recorded with a digital IR micropyrometer operating in the spectral range from 5.7 to 8.7 μm and measuring temperatures between 200 and 2000 °C in regions of size 0.5 – 5 mm with a response time of 0.1 s and a temperature measurement accuracy of ±10 °C [3].

The movement of the amorphisation front observed as the movement of the transparency front was studied by the methods of optical microscopy of sample sections and microvideo recording (video recording through a microscope [once the amorphisation (transparency) front achieved the bottom surface of samples).

Figure 4 shows the scheme of the experimental setup. The beam of a He – Ne laser was made coincident with the beam of a CO_2 laser to direct the latter. The CO_2 laser beam was focused by using a ZnSe lens with a focal distance of 12 cm. The irradiated region was illuminated by a fibre radiation source to observe it clearly in a microscope. The sample surface temperature and its variations in time were measured with a fast micropyrometer, and the amorphisation kinetics (the movement of the transparency front) was recorded with a video camera through another microscope.

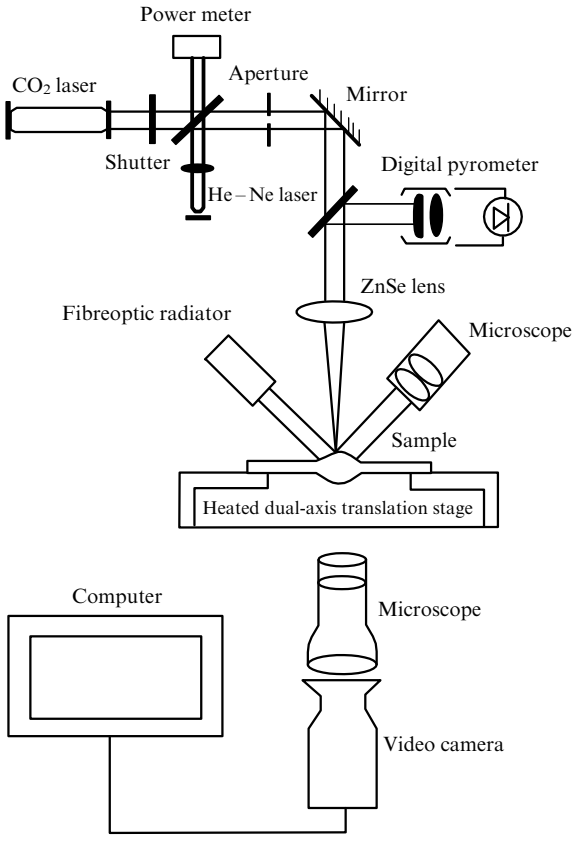

Figure 4. Scheme of the experimental setup.

3. Experimental results and discussion

Figure 5 presents typical curves of the sample-surface temperature variation during one heating–cooling cycle induced by radiation from a CO_2 laser with different power densities. In all cases, laser radiation should provide the sample surface heating up to a temperature of $\sim$1500 K exceeding the glass transition temperature $T_g = 1033$ K and the melting temperature $T_m = 1473$ K of sital.

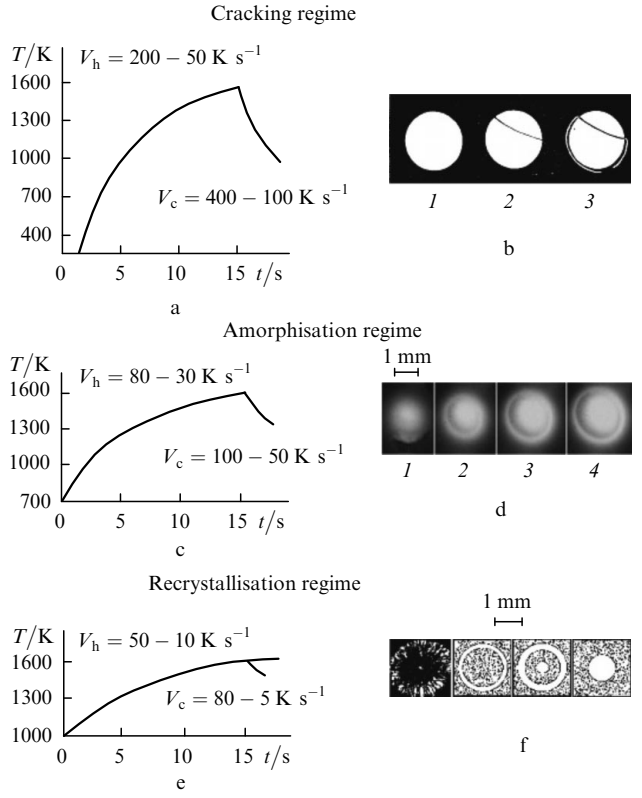

Figure 5. Temperature kinetics upon laser irradiation of ST-50-1 sital samples: heating–cooling rates (a, c, e) and corresponding visually observed structural changes (b, d, f) for samples of thickness $h = 0.6$ mm, the laser spot diameter $d_0 = 1 - 2$ mm, and the following irradiation parameters: the laser power density is $P = 10 - 15$ W, the power density is $q \geqslant 5 \times 10^6$ W m^{-2}, the initial temperature is $T_0 = 300$ K (a, b); $P = 1 - 3$ W, $q = 3 \times 10^5 - 1 \times 10^6$ W m^{-2}, $T_0 = 700$ K (c, d); and $P \leqslant 0.3$ W, $q \leqslant 10^5$ W m^{-2}, $T_0 = 1000$ K (e, f); (b) picture of cracks produced on the sample surface by laser irradiation [the sample view after 10 (*1*), 40 (*2*), and 90 s (*3*)]; (d) development of the amorphisation region during laser irradiation of the sample [video frames obtained within 6 (*1*), 6.5 (*2*), 7 (*3*), and 8 s (*4*) after the beginning of irradiation] and (f) the recrystallisation (and amorphisation) of the sample upon repeated irradiation by laser beams of different diameters (grey colour corresponds to the initial and recrystallised regions, white colour corresponds to the amorphous region); photographs and video frames were obtained in transmission.

In the first case (Fig. 5a), this temperature was achieved without any additional sample heating at laser power densities $(3 - 5) \times 10^6$ W m^{-2}. Under these conditions, cracks were produced in the irradiated region on the sample surface during exposure to laser radiation or more often after it (Fig. 5b).

At lower power densities ($10^5 - 10^6$ W m^{-2}) and preliminary heating of samples up to $T_0 = 700 - 900$ K (Fig. 5c), the GC amorphisation was observed in the irradiated region and samples became transparent, no cracks being produced (Fig. 5d).

As the laser power density was further decreased $q \leqslant 10^5$ W m^{-2} and samples were preliminary heated up to $T_0 = 800 - 1000$ K, the recrystallisation of irradiated (amorphous) samples was observed upon the repeated exposure to laser radiation, which in turn is also reversible (Fig. 5f).

As follows from the results presented above, the heating and cooling rates play a decisive role in the processes of local GC amorphisation and recrystallisation (Fig. 5).

The preliminary heating of samples is required to avoid the production of considerable thermal stresses, the formation of cracks, and the damage of samples. Thermal stresses are always produced upon local laser heating, especially when GCs, having rather low heat conduction, are irradiated. Local laser heating causes relatively high temperature gradients, which increase with increasing the heating temperature. Indeed, let us estimate roughly temperature gradients, by using the one-dimensional approximation grad $T = \partial T/\partial x$, which obviously gives the understated estimate. By replacing differentials by finite increments ΔT and Δx and assuming that $\Delta T \sim T_m - T_0 \approx 800 - 1200$ K (T_m is the melting temperature, T_0 is the sample heating temperature) and $\Delta x \approx \sqrt{a\tau}$ ($a = 6.5 \times 10^{-7}$ m^2 s^{-1} is the thermal diffusivity and $\tau \sim 1$ s is the laser irradiation time), we obtain considerable temperature gradients grad $T \sim \Delta T/\sqrt{a\tau} \approx 10^6$ K m^{-1}.

To avoid the laser-induced damage of GC samples, the two conditions should be fulfilled:

(i) The rate of temperature variation during heating and cooling should be lower than the critical rate V_T^{cr} (at which cracks are produced either during laser heating or subsequent cooling of a sample), i.e. laser-induced thermal stresses should not achieve the damage threshold [1];

(ii) the sample temperature should not exceed the vaporisation temperature T_v.

If the temperature variation rate exceeds the critical temperature ($V_T \geqslant V_T^{cr}$), cracks are inevitably produced (cracking regime). Upon processing of GCs in this regime, it is especially difficult to avoid the production of cracks due to residual stresses. One can see from Fig. 5b that a crack became noticeable already within 40 s and closed up within 90 c after the end of laser irradiation. This regime corresponds to the temperature kinetics in the ranges of heating rate $V_h \sim 200 - 50$ K s^{-1} and cooling rate $V_c \sim 400 - 100$ K s^{-1}.

At lower temperature variation rates $V_h \sim 30 - 80$ K s^{-1} and $V_c \sim 50 - 100$ K s^{-1}, the laser amorphisation of samples can be performed. In this case, the sample surface temperature achieves the melting temperature T_m, while the cooling rate is high enough for melt freezing and formation of an amorphous mass. The sample is melted in the irradiated region for a short time τ_m, which is necessary to heart the sample up to the temperature T_m [4]:

$$\tau_m = \frac{\pi k^2 (T_m - T_0)^2}{4q^2 a} \sim 1 \text{ s},$$

where $k = 1.45$ W m^{-1} K^{-1} is the GC heat conductivity; $T_0 = 800$ K; and $q = 10^6$ W m^{-2}. The melting front achieves the bottom surface of the sample after the time τ_h required for the through melting of plate of thickness h [4], where $\tau_h \approx 100h^2/4a$. For the sample thickness $h = 0.6$ mm, this time is $\tau_h \approx 6$ s. Beginning from this

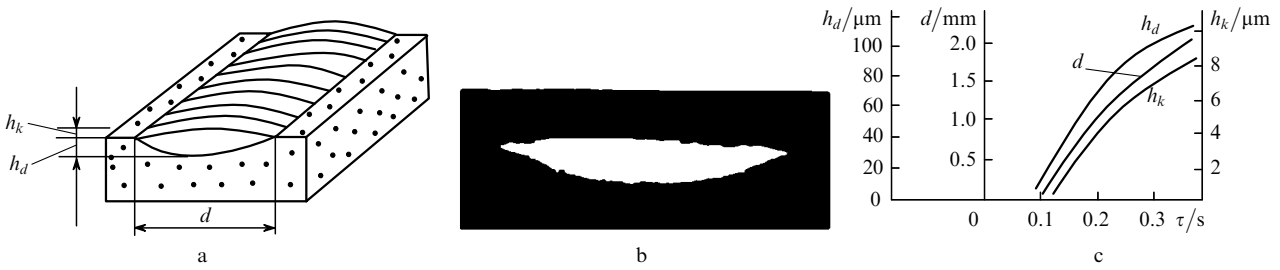

Figure 6. General view (a) and cross section (b) of a light guide and its formation kinetics (the initial amorphisation stage) (c): dependences of the height h_k, depth h_d, and width d of the light guide on the laser irradiation time $\tau = d_0/V_{sc}$ (V_{sc} is the scan time) for $d_0 = 1.5$ mm, $q = 0.5 \times 10^6$ W m^{-2} and $T_0 \approx 800$ K.

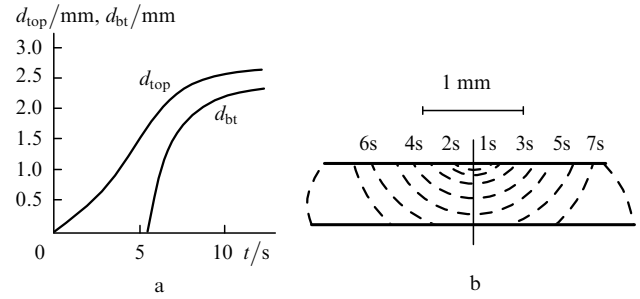

Figure 7. Dependences of the top (d_{top}) and bottom (d_{bt}) diameters of the lens on the laser irradiation time for $d_0 = 2$ mm, $h = 0.5$ mm, $q = 0.5 \times 10^6$ W m^{-2}, $T_0 \approx 800$ K (a) and the movement of the amorphisation front in the cross section recorded by using a microscope (b).

instant, the movement of the transparency front (amorphisation), which represents isotherm $T = T_m$, can be observed. After the end of laser irradiation, the amorphous structure is frozen due to the high cooling rate. The experimental time dependences of the dimensions of the amorphisation region are shown in Fig. 6c (depth and width) and Fig. 7 (top and bottom diameters). Figure 5d presents the video frames of the amorphous-region growth kinetics.

Laser amorphisation is also accompanied by some morphological changes in the irradiated region. Because the amorphous region has a lower density than the initial microcrystalline structure, the amorphisation region acquires the lens-like shape after laser irradiation due to the increase in the material macrovolume (Fig. 8c).

By summarising the above discussion, we note once more that the laser heating of GCs provides considerably higher rates of temperature variation (hundreds of kelvins per sec) compared to traditional heating methods (a few kelvins per sec). This new temperature kinetics in the case of LAGC makes it possible to develop a new method for manufacturing microoptical elements based on new optical materials.

4. Microoptical elements manufactured by LAGC

By using the laser amorphisation/crystallisation of GCs, a number of microoptical elements can be fabricated. Below, we list the parameters of these elements, which can be reliably controlled due to the unique properties of laser amorphisation:

(i) The element size can be controlled by varying the laser power density, the exposure time and temperature of the preliminary heating;

(ii) the element shape can be controlled by varying the shape and size of the irradiated region by the laser beam scan or with the help of projection masks;

(iii) the optical power (aperture) can be controlled by varying the sample thickness or a weighed portion of the same or different material;

(iv) optical properties (transmission, dispersion) can be controlled by varying the composition of the initial material.

Consider the main types of optical elements manufactured by us together with the group of P.A. Skiba [2].

4.1 Planar optical light guides and waveguides

By scanning a laser spot on the sample surface, we can fabricate planar optical light guides and waveguides with geometrical parameters determined by the scan rate and laser power density. The general view of such planar light guides is shown in Fig. 6a, the photograph of the cross section is presented in Fig. 6b, and the dependences of the height, depth, and width of light guides on the laser

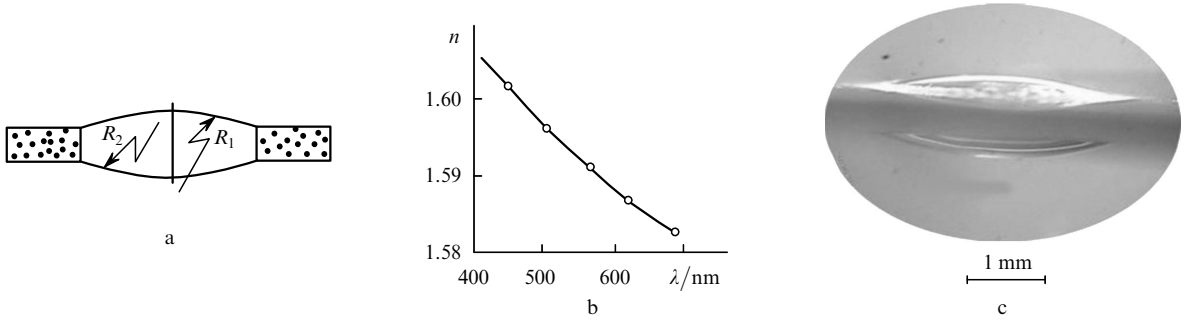

Figure 8. General view (a), dispersion curve (b), and photograph of a typical lens (c) fabricated by the LAGC method.

irradiation time are illustrated in Fig. 6c. The properties of planar light guides and waveguides are considered in detail in [2].

4.2 Lenses and lens arrays

Lenses are base elements in applied optics and find applications in most optical instruments. Traditional technologies for manufacturing optical lenses are well elaborated, but they are not applicable for fabricating miniature lenses of size no more than 1 mm [5]. The laser GC amorphisation is a new alternative method for manufacturing miniature lenses of diameters from tens of micrometres to a few millimetres. The range of focal distances of such lenses is rather broad (from a few centimetres down to one millimetre and smaller), and lenses with large apertures can be fabricated (NA = 0.6). In addition, all the fabrication processes are readily controlled and can be automated.

The general view of lenses manufactured by the LAGC method is presented in Fig. 8a, their dispersion and transmission are shown in Figs 8b and 2. Figure 7 shows the lens formation kinetics (changes in the top and bottom diameters of the lens and the movement of the transparency boundary).

The numerical aperture of such lenses is approximately 0.05 – 0.06. The aperture can be increased by placing an additional weighed portion of the same of different material to the irradiated region [2]. The weighed portion is melted during laser irradiation and is mixed with the material of the initial sample, by forming a common melt bath from which lenses with the larger radii of curvature of the top and bottom surfaces (i.e. with the larger aperture) are formed upon cooling. By using this method, the numerical aperture of lenses can be increased up to 0.1 – 0.6 and even more. Figure 9a presents the formation kinetics of a lens from a microscopic weighed portion obtained by the method of microvideo recording, and Fig. 9b demonstrated the dependence of the focal distance of lenses on the relative mass of the weighed portion of the same material. The calculated curve is plotted by using the radii of curvature of the top (R_1) and bottom (R_2) surfaces (see Fig. 8), which can be found from the balance equation $\sigma S_1/R_1 + mg/2 = \sigma S_2/R_2$ for forces, acting on the laser-irradiated region, and the law of conversion of mass $m_{am} = m_{cr} = m$, where σ is the surface tension of the melt; m is the melt mass; g is the gravitational constant; and S_1 and S_2 are the areas of the top and bottom melted surfaces.

By using proper masks, we can also fabricate lenses with different pupil configurations: elliptic, quadratic, etc. Figure 10 shows the schematic picture, photography, and profilograms of the elliptic lens sections.

The surfaces of lenses manufactured by LAGC are characterised by the atomic smoothness (see the Zygo interferogram in Fig. 11), and the quality of images produced by these lenses is illustrated by photographs obtained by using a raster of these lenses (Fig. 12).

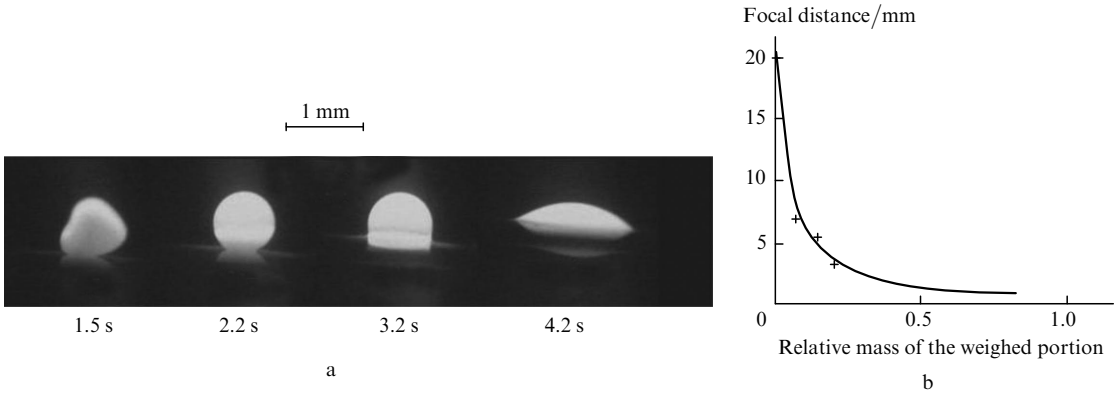

Figure 9. Kinetics of lens formation from a weighed portion (a) and dependence of the focal distance of lenses on the relative mass of the weighed portion (b) for $d_0 = 2$ mm, $h = 0.5$ mm, $q = 0.5 \times 10^6$ W m^{-2} and $T_0 \approx 800$ K; solid curve is calculations, crosses are experiment.

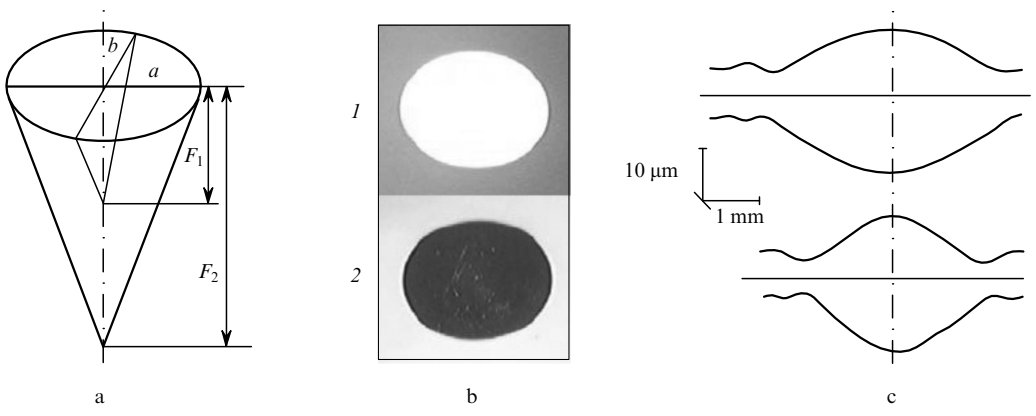

Figure 10. (a) Schematic picture of an ellipsoid-astigmatic lens (F_1 and F_2 are astigmatic focal segments); (b) photographs in transmitted (*1*) and reflected (*2*) light, (c) profilograms along the major (top) and minor (bottom) axes.

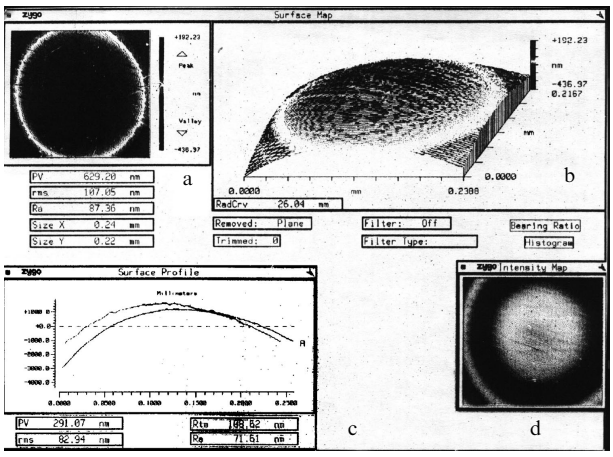

Figure 11. Surface parameters of a lens manufactured by the LAGC method measured with Zygo interferometer: general view (a), surface map (b), surface profile (c), and intensity distribution map (d).

4.3 Geodesic lenses

Geodesic, or planar, lenses are widely used in integrated optics to focus light in the lens plane (perpendicular to its optical axis). The image of one of such lenses is shown in Fig. 13b; Fig. 13c demonstrates the focusing of light, propagating in a planar waveguide, with the help of a geodesic lens.

4.4 Other optical elements

The LAGC method can be also used to fabricate many other optical elements. A combination of laser amorphisation followed by a partial crystallisation of the same region, but using a laser beam of different diameter, gives another new possibility to fabricate by this method various integral apertures (including apodized) and diffraction optical elements. The laser amorphisation/crystallisation of thin GC films can be also used in optical data storage.

5. Conclusions

(i) The amorphisation of GCs can be performed by exposing samples preliminary heated to 700–900 K (for ST-50-1) to the CO_2 laser radiation with a power density of $5 \times (10^5 - 10^6)$ W m^{-2}. The amorphisation kinetics is determined by the temperature kinetics, i.e. by the movement of the isotherm $T = T_m$ inside the irradiated region.

(ii) The laser radiation power density q required for amorphisation lies in the range $10^5 - 10^6$ W m^{-2}. At higher densities, GCs are cracked, while at lower densities no amorphisation occurs, but the recrystallisation of the corresponding glass (amorphous region) is observed upon its irradiation. The time τ_m required to initiate amorphisation (the time of sample heating up to temperature T_m) and time τ_h after which the amorphisation (melting) front achieves the lower surface of the sample are 0.1–1 and 1–10 s, respectively. These values strongly depend on the preliminary heating of samples.

(iii) Once the temperature of a GC sample surface achieves the melting temperature, scattering of light in the irradiated region strongly decreases due to the disappearance of boundaries between microcrystals during their melting. In this way the transparency front is formed, which penetrates inside the material in accordance with the temperature kinetics.

(iv) The produced high-temperature structure is frozen in the amorphisation regime after laser irradiation due to the rapid cooling rate $V_c = 50 - 100$ K s^{-1}, which is achieved owing to the heat conduction mechanism in the GC. The obtained amorphous phase can be recrystallised upon

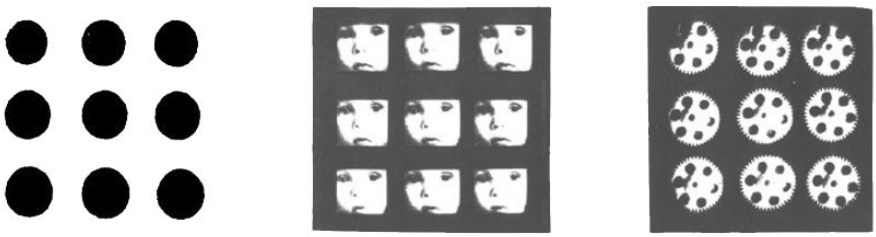

Figure 12. Miniature lens 3 × 3 raster fabricated by the LAGC method and photographs of objects obtained by using this raster (the plate thickness is $h = 0.6$ mm, $q \approx 2 \times 10^6$ W m^{-2}, $T_0 \approx 600$ K); the focal distance of lenses is $F = 21$ mm and its dispersion in the raster is $\Delta F = 3\,\%$.

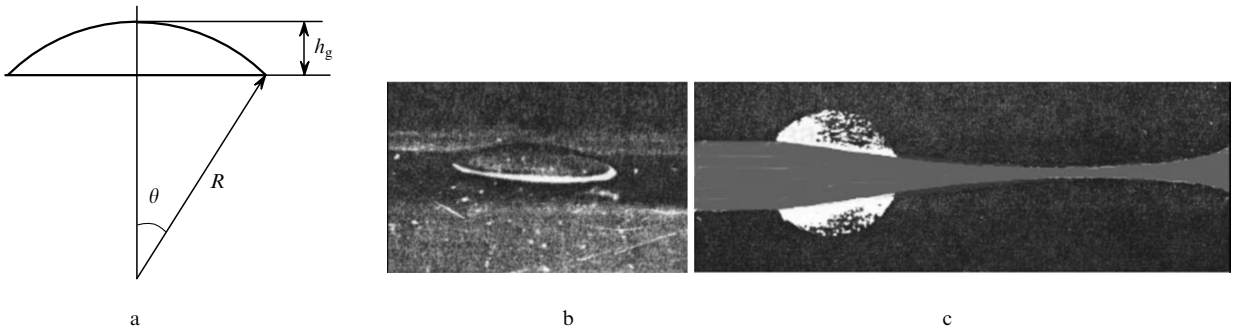

Figure 13. Schematic picture of a geodesic lens (h_g is the height, R is the radius of curvature, θ is the polar angle, $F = R(1 - \cos\theta)/2$) (a) and photographs of the lens profile (b) and light beam (top view) focused by the geodesic lens (c).

repeated irradiation [at lower power densities ($q < 10^5$ W m^{-2}) and correspondingly lower cooling rates ($V_c < 10 - 20$ K s^{-1})].

(v) The amorphous region obtained in the study represents a new optical material having all the properties of optical lenses: optical transparency in a broad wavelength range (from 0.3 to 4.5 μm for ST-50-1), the optical power due to the convex top and bottom surfaces, a broad range of possible numerical apertures (from 0.001 to 0.6), etc. The optical parameters of such lenses such as the numerical aperture, focal distance, diameter, pupil shape, etc. can be controlled by varying the laser power density, exposure time, laser spot size, aperture configuration, and the mass of an additional weighed portion.

(vi) Laser amorphisation/crystallisation can be used to fabricate various optical elements such as planar light guides and waveguides, lens rasters, aspheric and geodesic (planar) lenses, integral apertures, etc.

Further studies of laser amorphisation can lead to the creation of new optical materials, microscopic elements and devices.

Acknowledgements. This work was supported by the program of the President of the Russian Federation for Support of the Leading Scientific Schools (Grant No. NSh-5967.2006.8 'Fundamentals of Laser Microtechnologies') and he Russian Foundation for Basic Research (Grant No. 04-02-16611-a).

References

1. Veiko V.P., Yakovlev E.B. *Opt. Engineer.*, **33** (11), 3567 (1994).
2. Skiba P.A. *Lazernaya modifikatsiya steklovidnykh materialov* (Laser Modification of Glassy Materials) (Minsk: Belarussian State University, 1999).
3. Veiko V.P., Yakovlev E.B., et al. *Proc. SPIE Int. Soc. Opt. Eng.*, **1544**, 152 (1991).
4. Veiko V.P., Libenson M.N. *Lazernaya obrabotka* (Laser Machining) (Leningrad: Leniizdat, 1973).
5. Nussbaum Ph., Volkel R., Herzig H.P., Eisner M., Haselbeck S. *Pure Appl. Opt.*, **6**, 617 (1997).